DOI: 10.1002/ange.201403887

Paramagnetic Raman Optical Activity

Observation of Paramagnetic Raman Optical Activity of Nitrogen Dioxide**

Jaroslav Šebestík and Petr Bouř**

Abstract: *Raman optical activity (ROA) detects the intensity difference between right and left circularly polarized scattered light, and thus brings about enhanced information about the molecules under investigation. The difference is quite small and the technique is mostly constrained to the condensed phase. For NO_2 in the presence of a static magnetic field, however, the ROA signal with high ROA/Raman intensity ratio was observed. The signal is so strong owing to molecular paramagnetism and a pre-resonance signal enhancement. The spectral shape was explained on the basis of the Fermi golden rule and rotational wave functions expanded to a spherical top basis. The results indicate that the technique can be immediately used to obtain information about molecular properties, such as polarizability components. It also has a potential to detect other paramagnetic gases and discriminate among them.*

Chiral phenomena exploring different absorption or scattering of left and right circularly polarized light constantly attract attention because they provide enhanced information about molecules, most typically in the form of spectral bands differing in sign. Commonly used techniques include, for example, optical rotation and optical rotatory dispersion, dating back to the early career of Luis Pasteur,[1] electronic[2] and vibrational[3] circular dichroism, or vibrational Raman optical activity.[4] The traditional techniques inspire new methodologies, such as the cavity ring down polarimetry,[5] rotationally resolved vibrational circular dichroism,[6] or time-resolved experiments.[7]

It has been soon recognized that magnetic field must be taken into account to explain such experiments. For chiral, non-symmetrical molecules the magnetic component is provided by the motion of molecular electrons. But the magnetic field can also be imposed externally on an achiral sample,[8] giving rise to the family of magneto-optical phenomena, such as the Faraday effect or magnetic circular dichroism.[9]

Raman optical activity (ROA) is often more convenient than infrared techniques as it covers a wider part of the vibrational spectrum. It can be applied to small molecules as well as to large biopolymers and even viruses, and it benefits of a flexible experimental setup.[10] Typically, however, the ratio of the ROA to Raman intensity (traditionally referred to as CID, circular intensity difference) is very small, typically about 10^{-4}. Increasing the ROA signal or CID, for example, by surface enhanced scattering[11] or induced resonance[12] is often problematic and not suitable to a general sample. The ROA technique thus cannot be routinely applied to compounds in the gas phase, although recently we could measure ROA of methyloxirane vapor.[13]

Similarly, ROA of achiral samples kept in a static magnetic field is traditionally restricted to the condensed phase. It brought about useful information, for example, about metal complexes such as the ferrocytochrome c chromophore.[10a,14] Most (diamagnetic) gases only provide an immeasurably weak signal. However, the molecule of nitrogen dioxide enhances the measurement in two ways. First, it is paramagnetic; the free electron lends the molecule a magnetic moment, by several orders stronger than in the diamagnetic case. (The ratio is approximately given by the Bohr and nuclear magnetons, $\mu_B \approx 9.274 \times 10^{-24}\,\mathrm{J\,T^{-1}}$ vs. $\mu_N = 5.051 \times 10^{-27}\,\mathrm{J\,T^{-1}}$). Second, many NO_2 electronic levels pre-resonate with the impinging laser radiation, so that the overall Raman scattering and paramagnetic ROA (PROA) are very large.

Needless to say, NO_2 is one of the most common and most dangerous atmospheric pollutants. It is a commodity for making a wide range of products including explosives, fertilizers, and drugs. Atmospheric chemistry is affected by UV absorption on NO_2,[15] which can be studied, for example, by monitoring nitrogen isotopic ratios.[16] The 1995 Nobel Prize was awarded for the atmospheric chemistry of nitric oxide and nitrogen dioxide involved in ozone depletion.[17] The toxicity, comprising a destruction of epithelial cells in the lungs as the most immediate threat, has been documented in many studies.[18]

By a chance, nitrogen dioxide has amazingly complex spectra with a wealth of rotational, vibrational, and electronic levels, often described as chaotic.[19] Nevertheless, a large part of its rotational, vibrational, and electronic quantum chemistry has been elucidated,[20] and the spectra presented in our study are explicable on the basis of the angular momentum theory.[21]

We developed NO_2 chemically, then purified the gas and condensed it to a stock liquid. This proved convenient for relatively lengthy measurements, and for minimizing the effects of oxidation or laser light-induced decomposition. The commercial Biotools' ROA instrument based on the design of

---

[*] Dr. J. Šebestík, Prof. P. Bouř
Department of Molecular Spectroscopy, Institute of Organic Chemistry and Biochemistry, Academy of Sciences
Flemingovo náměstí 2, 166 10 Prague (Czech Republic)
E-mail: sebestik@uochb.cas.cz
bour@uochb.cas.cz

[**] The work was supported by the Academy of Sciences (grant number M200550902), Grant Agency of the Czech Republic (grant numbers P208/11/0105 and 14-00431S), and Ministry of Education (grant number LH11033). We thank Mr. Ondřej Pačes and Dr. Josef Kapitán for the help with the magnetic cell construction, and Dr. Radek Pelc for discussions on the manuscript.

Supporting information for this article is available on the WWW under http://dx.doi.org/10.1002/anie.201403887.

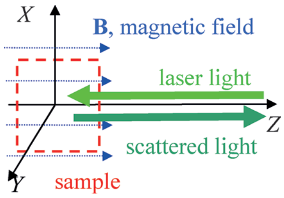

Figure 1. Geometry of the PROA experiment.

W. Hug and G. Hangartner[22] was expanded by the addition of a magnetic cell made of four neodymium magnets, providing a field of 1.5 tesla in the cell compartment. In the scattered circular polarized (SCP) backscattering experiment (Figure 1) the sample was irradiated by linearly polarized light, and the difference of the right and left circularly polarized scattered light ($I^R - I^L$) was detected.

Selected portions of ROA and Raman spectra are presented in Figure 2. The entire spectra can be found in the Supporting Information (Figure S2), together with experimental CID ratio and the degree of circularity, DOC. As pointed out previously,[23] depending on experimental conditions, pre-resonance Raman vibrational spectrum overlaps with fluorescence; occasionally the fluorescence may dominate. In our case, however, the vibrational components were much larger. The signal of the first fundamental mode ν_1, upper-left panel in Figure 2) is probably the most pronounced. Its Raman intensity is concentrated in the central "Q" band (around 750 cm^{-1}). Satellite rotational bands can be recognized as well, and modeled with reasonable accuracy even at the limited resolution and sensitivity of the single-monochromator spectrometer. Examples of the strongest Raman transitions contributing to the spectra are listed in Table S3 of SI. The ROA spectrum is dominated by a +/- "couplet" (close opposite bands) measured at 735/747 cm^{-1} and calculated at 746/753 cm^{-1}. It is followed by another couplet, experimentally at 778/782 cm^{-1}, calculated at 777/783 cm^{-1}. The intensity of rotational bands further away from the Q-band (for transitions involving large rotational quantum numbers, J) quickly fades and becomes undetectable.

The Raman and PROA signal of the ν_2 fundamental vibration centered around 1320 cm^{-1} is quite similar as for ν_1, which can be understood because of the same symmetry of these vibrations. On the other hand, the asymmetric N=O stretching vibration ν_3 around 1616 cm^{-1} provides a relatively weak Raman intensity, almost invisible at this scale, both in experiment and in theory. Interestingly, it does yield measurable ROA peaks (of "w"-shape, with extremes at 1603, 1625 and 1639 cm^{-1}, simulated at 1620, 1633, and 1644 cm^{-1}, respectively).

The most complex ROA signal appears within the 1400-1550 cm^{-1} interval. One can identify the combination band $2\nu_1$ at about 1500 cm^{-1}, where several rotational transitions can be assigned to the modeled Raman and ROA spectra. However, the relatively strong experimental Raman bands at 1518 and 1546 cm^{-1} seem to disturb the $2\nu_2$ signal, and most likely can be attributed to a fluorescence or coupling of electronic and vibrational levels (cf. also Figure S3). Finally,

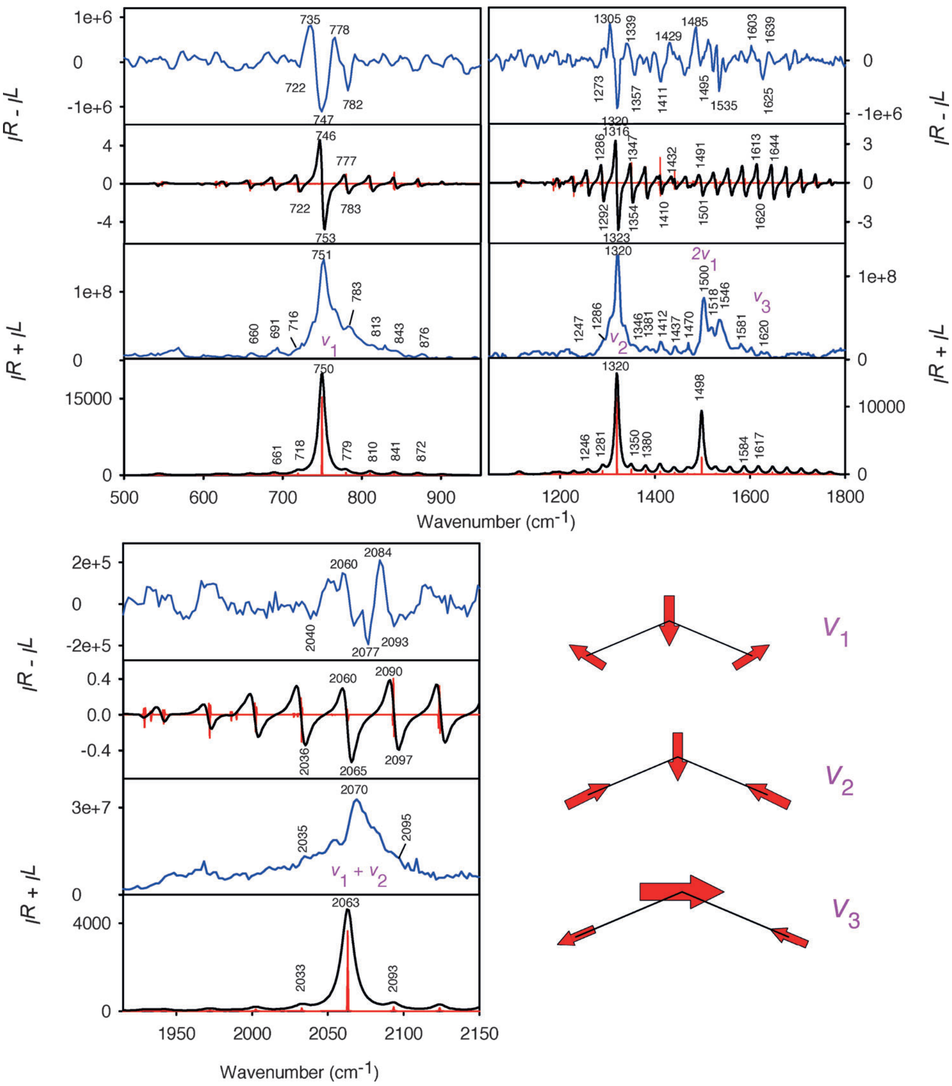

Figure 2. Experimental (blue) and simulated (black) PROA ($I^R - I^L$) and Raman ($I^R + I^L$) NO_2 spectra of the five vibrational transitions (ν_1, ν_2, ν_3, $2\nu_2$, $\nu_1+\nu_2$). The normal mode displacement for the three fundamentals is indicated as calculated at the B3LYP/6-311++G** level of approximation.

for the “isolated” $\nu_1+\nu_2$ combination transition at 2070 cm^{-1}, the Raman and ROA experimental spectra again appear to be fully explicable by the simulation, although the signal is relatively weak and more strongly affected by experimental noise than that of the ν_1 and ν_2 bands, for example. Still, the intensities of both the $2\nu_2$ and $\nu_1+\nu_2$ combination bands are remarkably strong, thus confirming a significant deviation of the vibrational potential of this molecule from the harmonic energy landscape.[20d]

The spectral shapes reflect contributions of individual polarizability components, as documented for the ν_1 signal in Figure 3. The transition polarizability[8,24] of this vibration is diagonal, with three non-zero components. As apparent from the figure, they generate very specific PROA spectral patterns that are easier to distinguish, at least by visual comparison, than the Raman intensity patterns. Note that the observed spectrum is not a simple sum of the three contributions. However, further improvement of experimental sensitivity is desirable for a more accurate experimental verification of the polarizability used in the modeling.

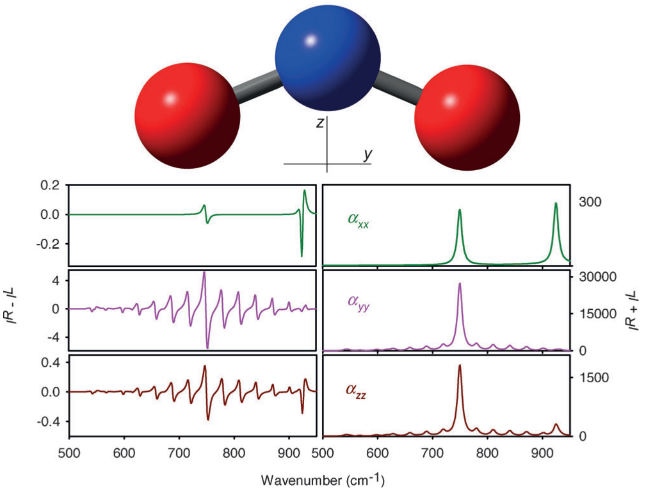

Figure 3. Simulated MROA (left) and Raman (right) NO_2 spectra of the ν_1 band, as obtained using three different diagonal parts of molecular transition polarizability (α_{xx}, α_{yy}, and α_{zz}).

A more applied potential of PROA for analyzing the nitrogen paramagnetic gases is illustrated in Figure 4 where we encountered an increased sensitivity of this technique to the impurities (NO, N_2O_4, N_2O_3, etc.) in the NO_x mixture[25] compared to the pure NO_2 sample. In particular, the 1350-1430 cm^{-1} region in PROA is clearly affected by the impurities, whereas the Raman scattering remains almost undisturbed. The band at 1320 cm^{-1} itself does not seem to be significantly perturbed, ν_1 band around 750 cm^{-1} significantly changes its shape, and a new negative PROA signal at 642 cm^{-1} appears for NO_x.

We can thus conclude that the magnetic Raman optical activity of the NO_2 molecule could be observed for all three fundamental and two combination transitions, and that the angular momentum theory could explain fine spectral features reasonably well, within the limit of experimental resolution and noise. The possibility to relate the spectra to molecular polarizability, and the generally higher sensitivity of PROA to the system chemistry indicate a tremendous potential of the PROA spectroscopy in analytical chemistry of the nitric dioxide and other paramagnetic gases.

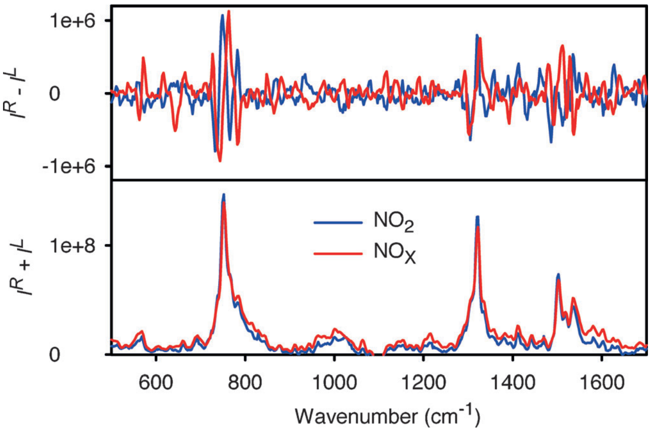

Figure 4. ROA and Raman spectra of pure NO_2 (blue) and the NO_x mixture (red).

Received: April 1, 2014

Keywords: angular momentum theory · nitrogen dioxide · paramagnetic gases · Raman optical activity · spectral simulations

[1] L. Pasteur, *Théses de chimie et de physique*, Bachelier, Paris, **1847**.
[2] R. W. Woody, *Adv. Biophys. Chem.* **1992**, *2*, 37–79.
[3] G. Holzwarth, E. C. Hsu, H. S. Mosher, T. R. Faulkner, A. Moscowitz, *J. Am. Chem. Soc.* **1974**, *96*, 251–252.
[4] a) L. D. Barron, M. P. Bogaard, A. D. Buckingham, *J. Am. Chem. Soc.* **1973**, *95*, 603–605; b) J. Haesler, I. Schindelholz, E. Riguet, C. G. Bochet, W. Hug, *Nature* **2007**, *446*, 526–529.
[5] T. Müller, K. B. Wiberg, P. H. Vaccaro, *J. Phys. Chem. A* **2000**, *104*, 5959–5968.
[6] B. Wang, P. Bouř, T. A. Keiderling, *Phys. Chem. Chem. Phys.* **2012**, *14*, 9586–9593.
[7] H. Rhee, Y. G. June, J. S. Lee, K. K. Lee, J. H. Ha, Z. H. Kim, S. J. Jeon, M. Cho, *Nature* **2009**, *458*, 310–313.
[8] L. D. Barron, *Molecular Light Scattering and Optical Activity*, Cambridge University Press, Cambridge, **2004**.
[9] a) P. J. Stephens, *J. Chem. Phys.* **1970**, *52*, 3489–3516; b) G. H. Wagnière, *Chem. Phys.* **1999**, *245*, 165–173; c) L. D. Barron, A. D. Buckingham, *Mol. Phys.* **1972**, *23*, 145–150.
[10] a) L. D. Barron, L. Hecht, I. H. McColl, E. W. Blanch, *Mol. Phys.* **2004**, *102*, 731–744; b) L. Nafie, *Vibrational optical activity: Principles and applications*, Wiley, Chichester, **2011**.
[11] a) S. Abdali, *J. Raman Spectrosc.* **2006**, *37*, 1341–1345; b) K. Osińska, M. Pecul, A. Kudelski, *Chem. Phys. Lett.* **2010**, *496*, 86–90.
[12] S. Yamamoto, P. Bouř, *Angew. Chem.* **2012**, *124*, 11220–11223; *Angew. Chem. Int. Ed.* **2012**, *51*, 11058–11061.
[13] J. Šebestík, P. Bouř, *J. Phys. Chem. Lett.* **2011**, *2*, 498–502.
[14] a) L. D. Barron, J. Vrbancich, *J. Raman Spectrosc.* **1983**, *14*, 118–125; b) L. D. Barron, C. Meehan, J. Vrbancich, *J. Raman Spectrosc.* **1982**, *12*, 251–261.

[15] H. Okabe, *The photochemistry of small molecules*, Wiley, New York, **1978**.
[16] E. C. Zipf, S. S. Prasad, *Science* **1998**, *279*, 211–213.
[17] P. J. Crutzen, *Annu. Rev. Earth Planet. Sci.* **1979**, *7*, 443–472.
[18] N. M. Elsayed, *Toxicology* **1994**, *89*, 161–174.
[19] a) R. Georges, A. Delon, R. Jost, *J. Chem. Phys.* **1995**, *103*, 1732–1747; b) S. L. Coy, K. K. Lehmann, F. C. DeLucia, *J. Chem. Phys.* **1986**, *85*, 4297–4304; c) K. K. Lehmann, S. L. Coy, *J. Chem. Phys.* **1985**, *83*, 3290–3296.
[20] a) C. C. Lin, *Phys. Rev.* **1959**, *116*, 903–910; b) W. J. Lafferty, R. L. Sams, *J. Mol. Spectrosc.* **1977**, *66*, 478–492; c) A. Perrin, C. Camy-Peyret, J. M. Flaud, *J. Mol. Spectrosc.* **1988**, *130*, 168–182; d) A. Perrin, J. M. Flaud, C. Camy-Peyret, A. M. Vasserot, G. Guelachvili, A. Goldman, F. J. Murcray, R. D. Blatherwick, *J. Mol. Spectrosc.* **1992**, *154*, 391–406; e) Y. Liu, X. Liu, H. Liu, Y. Guo, *J. Mol. Spectrosc.* **2000**, *202*, 306–308.
[21] a) L. D. Barron, C. J. Johnston, *J. Raman Spectrosc.* **1985**, *16*, 208–218; b) R. N. Zare, *Angular Momentum*, Wiley, New York, **1988**.
[22] W. Hug, G. Hangartner, *J. Raman Spectrosc.* **1999**, *30*, 841–852.
[23] M. J. Marsden, G. R. Bird, *J. Chem. Phys.* **1973**, *59*, 2766–2767.
[24] S. Yamamoto, P. Bouř, *J. Comput. Chem.* **2013**, *34*, 2152–2158.
[25] P. Gray, A. D. Yoffe, *Chem. Rev.* **1955**, *55*, 1069–1154.